



ELSEVIER

Nuclear Instruments and Methods in Physics Research A 464 (2001) 358–368

**NUCLEAR
INSTRUMENTS
& METHODS
IN PHYSICS
RESEARCH**
Section A

www.elsevier.nl/locate/nima

Analytical and nonlinear perturbative simulation studies of the equilibrium and stability properties of intense charged particle beams for heavy ion fusion[☆]

Ronald C. Davidson*, Hong Qin, W. Wei-li Lee, Sean Strasburg

Plasma Physics Laboratory, Princeton University Princeton, New Jersey, NJ 08543, USA

Abstract

This paper presents an overview of recent analytical and numerical investigations of collective processes in intense ion beams at the Plasma Physics Laboratory based on the nonlinear Vlasov–Maxwell equations. The topics covered include: (a) nonlinear stability theorem for quiescent beam propagation at high space-charge intensities; (b) development and application of Hamiltonian averaging techniques for intense beam propagation through alternating-gradient field configurations; (c) kinetic studies of the electron–ion two-stream instability which occurs when an (unwanted) component of electrons is present in the beam transport line; (d) application of the newly developed three-dimensional, multispecies, nonlinear perturbative particle simulation scheme, called the Beam Equilibrium, Stability and Transport (BEST) code, to investigate the linear and nonlinear dynamics of intense beam propagation, including the electron–ion two-stream instability; and (e) investigations of the role of collective mode excitations in the expulsion of particles from the beam core and the production of halo particles. Finally, the linear growth properties of instabilities driven by pressure anisotropy are investigated within the framework of a macroscopic warm-fluid model. © 2001 Elsevier Science B.V. All rights reserved.

0. Introduction

Periodic focusing accelerators and transport systems [1–8] have a wide range of applications ranging from basic scientific research in high energy and nuclear physics, to applications such as heavy ion fusion, spallation neutron sources, tritium production, and nuclear waste treatment, to mention a few examples. Of particular interest, at the high beam currents and charge densities of practical interest, are the combined effects of the applied focusing field and the intense self-fields

produced by the beam space charge and current on determining detailed equilibrium, stability, and transport properties [1–3]. Through basic experimental studies, analytical investigations based on the nonlinear Vlasov–Maxwell equations, and numerical simulations using particle-in-cell models and nonlinear perturbative simulation techniques, considerable progress has been made in developing an improved understanding of the collective processes and nonlinear beam dynamics characteristic of high-intensity beam propagation [9–38] in periodic focusing and uniform focusing transport systems. Nonetheless, it remains important to develop an improved basic understanding of the nonlinear dynamics and collective processes in periodically focused intense charged particle

[☆]Research supported by the U.S. Department of Energy.

*Corresponding author. Fax: +1-609-243-2749.

E-mail address: rdavidson@pppl.gov (R.C. Davidson).

beams, with the goal of identifying operating regimes for stable (quiescent) beam propagation over hundreds, even thousands, of lattice periods of the periodic focusing magnetic field, including a minimum degradation of beam quality and luminosity.

This paper presents a brief summary of selected heavy ion fusion research activities carried out at the Princeton Plasma Physics Laboratory since the 1997 Heidelberg symposium on heavy ion fusion [7], with particular emphasis on analytical and numerical simulation studies of collective processes in intense beam propagation. The work summarized here includes: development of a three-dimensional stability theorem for intense beam propagation based on the nonlinear Vlasov–Maxwell equations (Section 1); analytical and numerical studies of the electron–ion two-stream instability in high-intensity ion beams (Section 2); warm-fluid investigations of collective instabilities driven by pressure anisotropy in intense charged particle beams (Section 3); studies of halo particle production by collective mode excitations (Section 4); and the development of Hamiltonian averaging techniques for describing intense beam propagation through periodic focusing field configurations (Section 5).

1. Three-dimensional kinetic stability theorem for high-intensity beam propagation

In a recent calculation [18,19], global conservation constraints obtained from the nonlinear Vlasov–Maxwell equations have been used to derive a three-dimensional kinetic stability theorem for an intense nonneutral ion beam (or charge bunch) propagating in the z -direction with average axial velocity $V_b = \beta_b c = \text{const.}$ and characteristic kinetic energy $(\gamma_b - 1)m_b c^2$ in the laboratory frame. The particle motion in the beam frame (‘primed’ coordinates) is assumed to be nonrelativistic, and the beam is assumed to have sufficiently high directed axial velocity that $V_b \gg |\mathbf{v}'|$. Space-charge effects and transverse electromagnetic effects are incorporated in the analysis in a fully self-consistent manner. The nonlinear Vlasov–Maxwell equations are Lorentz-transformed to

the beam frame, and the applied focusing potential is assumed to have the (time-stationary) form in the smooth-focusing approximation

$$\psi'_{\text{sf}}(\mathbf{x}') = \frac{1}{2}\gamma_b m_b [\omega_{\beta\perp}^2 (x'^2 + y'^2) + \omega_{\beta z}^2 z'^2] \quad (1)$$

where $\omega_{\beta\perp}$ and $\omega_{\beta z}$ are constant focusing frequencies. Using global conservation constraints satisfied by the nonlinear Vlasov–Maxwell equations, it is shown [18] that a sufficient condition for linear and nonlinear stability for perturbations with arbitrary polarization about a beam equilibrium distribution $f_{\text{eq}}(\mathbf{x}', \mathbf{p}')$ is that f_{eq} be a monotonically decreasing function of the single-particle energy H' in the beam frame, i.e.

$$\frac{\partial}{\partial H'} f_{\text{eq}}(H') \leq 0. \quad (2)$$

Here, H' is defined by

$$H' = \frac{1}{2m_b} \mathbf{p}'^2 + \psi'_{\text{sf}}(\mathbf{x}') + q_b \phi'_{\text{eq}}(\mathbf{x}') \quad (3)$$

where $\phi'_{\text{eq}}(\mathbf{x}')$ is the space-charge potential. This theorem represents a very powerful result since it identifies the class of beam distribution functions that can propagate quiescently over large distances. Most notably, it applies to perturbations about beam equilibria $f_{\text{eq}}(H')$ with arbitrary wave polarization and initial amplitude; to continuous beams that are radially confined and infinite in axial extent ($\omega_{\beta\perp} \neq 0$, $\omega_{\beta z} = 0$); to charge bunches that are radially and axially confined ($\omega_{\beta\perp} \neq 0$ and $\omega_{\beta z} \neq 0$); and to beams with arbitrary space-charge intensity consistent with the applied focusing potential $\psi'_{\text{sf}}(\mathbf{x}')$ providing confinement of the beam particles. The nonlinear stability theorem [18] embodied in Eqs. (2) and (3) represents a major generalization of the stability theorem first developed by Newcomb and Gardner for perturbations about a spatially uniform, charge-neutral plasma, and extended by Davidson and Krall to the case of electrostatic nonneutral plasma column [19].

Recently, the δf formalism, a low-noise, nonlinear perturbative particle simulation technique, has been developed for intense beam applications, and applied to matched-beam propagation in a periodic focusing field [20–22] and other related studies. Using the newly developed Beam Equilibrium, Stability and Transport (BEST) code

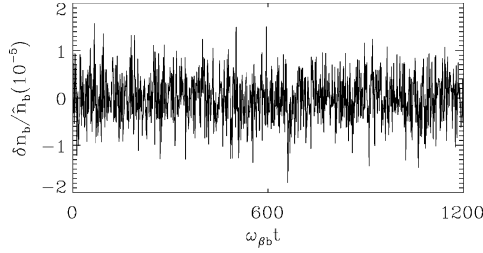


Fig. 1. Time history of $\delta n_b / \bar{n}_b$ for small-amplitude perturbations about a thermal equilibrium ion beam.

[39–41], a 3D multispecies, nonlinear perturbative simulation code, we have tested the nonlinear stability theorem in Eq. (2) for the particularly choice of a thermal equilibrium distribution $f_{\text{eq}}(H') = \beta \exp(-H'/T_b)$, where β and T_b are positive constants, and $\omega_{\beta z} = 0$ is assumed (continuous beam in the axial direction). Typical simulation results [41] are illustrated in Fig. 1, where initial low-level noise in the perturbed density, $\delta n_b = \int d^3p \delta f_b$ is introduced at $t = 0$, and the simulations show that the beam propagates quiescently over 1200 equivalent lattice periods. The system parameters assumed in Fig. 1 are $\gamma_b = 1.08$, mass number $A = 133$ (Cesium ions), and $\hat{\omega}_{\beta b}^2 / 2\gamma_b^2 \omega_{\beta \perp}^2 = 0.95$, where $\hat{\omega}_{\beta b}^2 = 4\pi \hat{n}_b q_b^2 / \gamma_b m_b$ is the on-axis ($r = 0$) plasma frequency-squared.

2. Kinetic description of electron–ion two-stream instability in high-intensity ion beams

For a one-component high-intensity beam, considerable progress has been made in describing the self-consistent evolution of the beam distribution function $f_b(\mathbf{x}, \mathbf{p}, t)$ and the self-generated electric and magnetic fields in kinetic analyses [4–26] based on the Vlasov–Maxwell equations. In many practical accelerator applications, however, an (unwanted) second charge component is present. For example, a background population of electrons can result by secondary emission when energetic beam ions strike the chamber wall, or through ionization of background neutral gas by the beam ions. When a second charge component is present, it has been recognized for many years, both in theoretical studies and in experimental

observations [27,28,42,43], that the relative streaming motion of the high-intensity beam particles through the background charge species provides the free energy to drive the classical two-stream instability, appropriately modified to include the effects of dc space charge, relativistic kinematics, presence of a conducting wall, etc. A well-documented example is the electron–proton two-stream instability observed in the Proton Storage Ring [27,28,37], although a similar instability also exists for other ion species, including (for example) electron–ion interactions in electron storage rings [29–34].

In a recent analysis [42,43], we have made use of the Vlasov–Maxwell equations to develop a fully kinetic description of the electron–ion two-stream instability driven by the directed axial motion of a high-intensity ion beam propagating in the z -direction with average axial momentum $\gamma_b m_b \beta_b c$ through a stationary population of background electrons. The ion beam has characteristic radius r_b and is treated as continuous in the z -direction, and the applied transverse focusing force on the beam ions is modeled by $F_{\text{foc}}^b = -\gamma_b m_b \omega_{\beta b}^2 \mathbf{x}_\perp$ in the smooth-focusing approximation. Here, $\omega_{\beta b} = \text{const.}$ is the effective betatron frequency associated with the applied focusing field, \mathbf{x}_\perp is the transverse displacement from the beam axis, $(\gamma_b - 1)m_b c^2$ is the ion kinetic energy, and $V_b = \beta_b c$ is the average axial velocity, where $\gamma_b = (1 - \beta_b^2)^{-1/2}$ is the relativistic mass factor. Furthermore, the ion motion in the beam frame is assumed to be nonrelativistic, and the electron motion in the laboratory frame is assumed to be nonrelativistic. The ion charge and number density are denoted by $q_b = Z_b e$ and n_b , and the electron charge and number density by $-e$ and n_e . For $Z_b n_b > n_e$, the electrons are electrostatically confined in the transverse direction by the space-charge potential ϕ produced by the excess ion charge. The equilibrium and stability analysis retains the effects of finite radial geometry transverse to the beam propagation direction, including the presence of a perfectly conducting cylindrical wall located at radius $r = r_w$. In addition, the analysis assumes perturbations with long axial wavelength

$$k_z^2 r_b^2 \ll 1. \quad (4)$$

We introduce the ion plasma frequency-squared defined by $\hat{\omega}_{pb}^2 = 4\pi\hat{n}_b Z_b^2 e^2 / \gamma_b m_b$, and the fractional charge neutralization defined by $f = \hat{n}_e / Z_b \hat{n}_b$, where \hat{n}_b and \hat{n}_e are the characteristic ion and electron densities. The equilibrium and stability analysis is carried out for *arbitrary* normalized beam intensity $\hat{\omega}_{pb}^2 / \omega_{\beta b}^2$, and *arbitrary* fractional charge neutralization f , consistent with radial confinement of the beam particles.

For the moderately high beam intensities envisioned in the proton linacs and storage rings for the Spallation Neutron Source, the normalized beam intensity is typically $\hat{\omega}_{pb}^2 / 2\gamma_b^2 \omega_{\beta b}^2 \lesssim 0.1$. Typical numerical results [41] using the BEST non-linear perturbative simulation code are illustrated in Fig. 2 for the case of an intense proton beam with $\gamma_b = 1.85$, $\hat{\omega}_{pb}^2 / 2\gamma_b^2 \omega_{\beta b}^2 = 0.074$, and $T_{b\perp} / \gamma_b m_b V_b^2 = 3.61 \times 10^{-6}$, propagating through stationary background electrons with $V_e = 0$, $T_{e\perp} / \gamma_b m_b V_b^2 = 5.86 \times 10^{-7}$, and fractional charge neutralization $f = \hat{n}_e / \hat{n}_b = 0.1$. Note from Fig. 2 that the $x-y$ projection of the perturbed space-charge potential $\delta\phi(x, y, z, t)$ develops a strong dipole ($\ell = 1$) feature during the exponential growth phase, which is consistent with analytical predictions [42,43]. The ions and electrons are taken to be initially cold in the axial direction ($v_{Tbz} = 0 = v_{Tez}$) for the simulation shown in Fig. 2.

For heavy ion fusion applications, however, the transverse beam emittance is very small, and the space-charge-dominated beam intensity is much larger, with $\hat{\omega}_{pb}^2 / 2\gamma_b^2 \omega_{\beta b}^2 \lesssim 1$. The stability analysis shows [42,43] that the instability growth rate $\text{Im } \omega$ increases with increasing normalized beam intensity $\hat{\omega}_{pb}^2 / \omega_{\beta b}^2$, and increasing fractional charge neutralization f . In addition, the instability is strongest (largest growth rate) for perturbations with azimuthal mode number $\ell = 1$, corresponding to a simple (dipole) transverse displacement of the beam ions and the background electrons. For the case of overlapping step-function density profiles for the beam ions and background electrons, corresponding to monoenergetic ions and electrons in the transverse direction, a key result is that there is no threshold in beam intensity or fractional charge neutralization for the onset of instability in circumstances where the beam ions

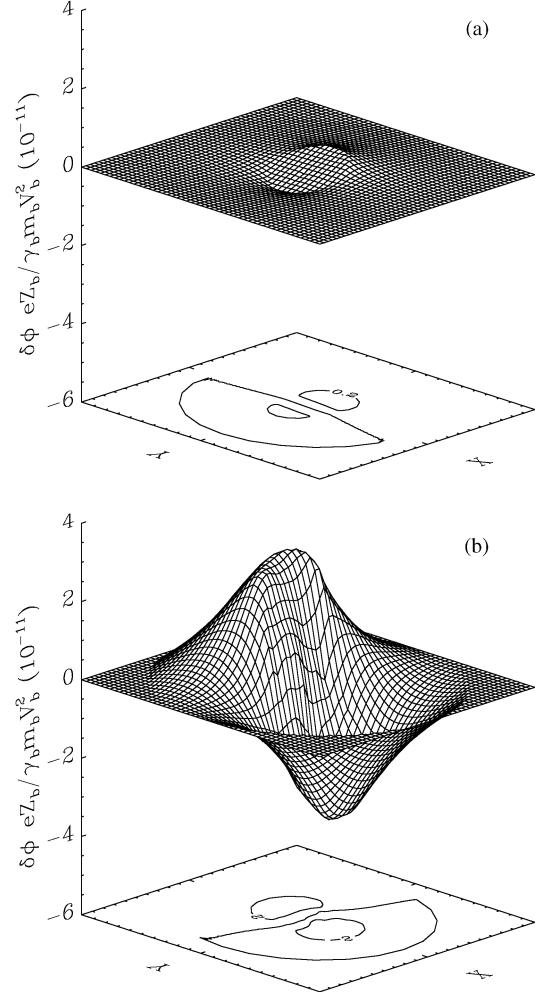


Fig. 2. The $x-y$ projection (at fixed value of z) of the perturbed electrostatic potential $\delta\phi(x, y, t)$ for the electron-ion two-stream instability growing from a small initial perturbation, shown at (a) $t = 0$, and (b) $\omega_{\beta b} t = 200$.

are ‘cold’ in the axial direction (negligible axial momentum spread). On the other hand, introduction of a small axial momentum spread Δp_{zj} can be sufficient to stabilize the two-stream instability by longitudinal Landau damping effects [44,45]. This is illustrated in Fig. 3, where the unstable solution to the quartic dispersion relation obtained from the linearized Vlasov–Maxwell equations [45] is plotted for system parameters corresponding to $\hat{\omega}_{pb}^2 / 2\gamma_b^2 \omega_{\beta b}^2 = 0.98$, $Z_b = 1$, $A = 133$ (cesium

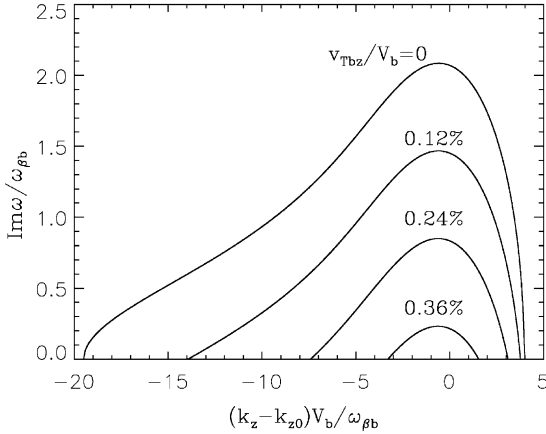


Fig. 3. Plots of (a) normalized growth rate $\text{Im } \omega / \omega_{\beta b}$ versus shifted axial wavenumber $(k_z - k_{z0}) V_b / \omega_{\beta b}$ obtained from the kinetic dispersion relation for the unstable branch with positive real frequency. System parameters correspond to $\omega_{pb}^2 / 2\gamma_b^2 \omega_{\beta b}^2 = 0.98$, $v_{Tez} = v_{Tbz}$, $Z_b = 1$, $A = 133$ (cesium ions), $(\gamma_b - 1)m_b c^2 = 4.5$ GeV, $r_b/r_w = 0.5$, and $f = 0.1$. Curves are shown for several values of normalized ion thermal spread v_{Tbz}/V_b ranging from 0 to 0.01.

ions), $(\gamma_b - 1)m_b c^2 = 4.5$ GeV, $r_b/r_w = 0.5$, $f = 0.1$, and several values of $v_{Tbz}/V_b = \Delta p_{zb}/\gamma_b m_b V_b$ ranging from 0 to 0.01. In Fig. 3, the normalized growth rate $\text{Im } \omega / \omega_{\beta b}$ is plotted versus normalized axial wavenumber $(k_z - k_{z0}) V_b / \omega_{\beta b}$, and we have taken $v_{Tez} = v_{Tbz}$ for purposes of illustration. Note from Fig. 3 that a relatively small axial momentum spread is adequate to stabilize the electron–ion two-stream instability by longitudinal Landau damping effects. If the beam ions and background electrons are initially cold axially, then a likely nonlinear consequence of the instability would be to cause an increase in axial momentum spread, thereby leading to a stabilization of the instability by parallel kinetic effects.

3. Warm-fluid description of collective instabilities driven by pressure anisotropy in intense charged particle beams

In general, a complete description of collective processes in intense nonneutral beams requires a knowledge of the beam distribution function $f_b(\mathbf{x}, \mathbf{p}, t)$ in the six-dimensional phase space (\mathbf{x}, \mathbf{p}) ,

in order to carry out numerical simulations using the distribution function as an initial condition, or to carry out analytical studies of kinetic equilibrium and stability behavior. While considerable progress has been made in analytical investigations based on the Vlasov–Maxwell equations [9–19], such kinetic analyses are often complex, even under idealized assumptions. It is therefore important to develop and test the robustness of alternative theoretical models, such as macroscopic models [46–49]¹ based on the fluid–Maxwell equations, for investigating beam equilibrium and stability properties. Such macroscopic fluid descriptions have met with recent success in describing the propagation of space-charge-dominated (low-emittance) beams in periodic-focusing transport systems [46,49], and in describing high-frequency collective oscillations in high-intensity beams [48]. In a recent calculation [50], we make use of the macroscopic warm-fluid model developed by Lund and Davidson [48] in the smooth-focusing approximation to investigate the linear stability properties of an intense charged particle beam, allowing for equilibrium pressure anisotropy ($P_{\perp}^0 \neq P_{\parallel}^0$). A particular focus of the analysis [50] is application of the warm-fluid model to investigate the anisotropy-driven ($P_{\perp}^0 > P_{\parallel}^0$) instability observed in particle-in-cell simulations and studied analytically using the Vlasov–Maxwell equations [51,52]. Such anisotropies are well known to develop naturally in accelerators, and can provide the free energy to drive instabilities and cause a deterioration in beam quality and emittance.

To briefly summarize the assumptions and macroscopic warm-fluid model applied in the stability studies [50], the characteristic beam radius is denoted by r_b , and it is assumed that the particle motion in the beam frame is nonrelativistic. Transverse confinement of the beam particles is provided by applied magnetic or electric focusing fields, and in the *smooth-focusing* approximation

¹ Ref. [1] presents a general derivation of the macroscopic fluid Maxwell equations from the Vlasov–Maxwell equations on pp. 22–26. Several aspects of cold-fluid equilibrium and stability properties of nonneutral beam-plasma systems are described on pp. 240–276 of Ref. [1].

we model the applied transverse focusing force on a beam particle by $\mathbf{F}_{\text{foc}} = -\gamma_b m \omega_{\beta b}^2 (x \hat{\mathbf{e}}_x + y \hat{\mathbf{e}}_y)$, where $\omega_{\beta b} = \text{const.}$ is the effective betatron frequency for the transverse oscillations, and (x, y) is the transverse displacement from the beam axis. Following Lund and Davidson [48], by taking appropriate momentum moments of the nonlinear Vlasov equation for the beam distribution function $f_b(\mathbf{x}, \mathbf{p}, t)$ in the six-dimensional phase space (\mathbf{x}, \mathbf{p}) , we obtain an interconnected chain of macroscopic fluid equations advancing the particle density $n(\mathbf{x}, t)$, the average flow velocity $\mathbf{V}(\mathbf{x}, t) = V_z(\mathbf{x}, t) \hat{\mathbf{e}}_z + \mathbf{V}_\perp(\mathbf{x}, t)$, the pressure tensor $\mathbf{P}(\mathbf{x}, t)$, the heat flow tensor $\mathbf{Q}(\mathbf{x}, t)$, etc. In the present analysis, we adopt a model¹ in which the heat-flow contribution, proportional to $(\partial/\partial \mathbf{x}) \cdot \mathbf{Q}(\mathbf{x}, t)$, is neglected in the dynamical equation advancing the pressure tensor $\mathbf{P}(\mathbf{x}, t)$, thereby leading to a closed system of macroscopic fluid-Maxwell equations describing beam equilibrium and stability properties. In addition, the pressure tensor $\mathbf{P}(\mathbf{x}, t)$ is assumed to be isotropic in the plane perpendicular to the beam propagation direction (the z -direction), i.e., $\mathbf{P}(\mathbf{x}, t) = P_\perp(\mathbf{x}, t)(\hat{\mathbf{e}}_x \hat{\mathbf{e}}_x + \hat{\mathbf{e}}_y \hat{\mathbf{e}}_y) + P_\parallel(\mathbf{x}, t) \hat{\mathbf{e}}_z \hat{\mathbf{e}}_z$, where $P_\perp(\mathbf{x}, t)$ and $P_\parallel(\mathbf{x}, t)$ are scalar pressures. Finally, under axisymmetric equilibrium conditions with $\partial/\partial \theta = 0$, $\partial/\partial t = 0$ and $\partial/\partial z = 0$, the warm fluid-Maxwell equations support a broad class of solutions for the equilibrium density and pressure profiles $n^0(r)$, $P_\perp^0(r)$, and $P_\parallel^0(r)$. In the analysis, we limit the detailed investigations of stability behavior for small-amplitude perturbations to the class of so-called *waterbag* equilibria [14,16] in which $P_\perp^0(r) = \text{const.}[n^0(r)]^2$ and $P_\parallel^0(r) = \text{const.}[n^0(r)]$. The stability analysis allows for general pressure anisotropy, permitting a detailed investigation of anisotropy-driven instabilities when $P_\perp^0 > P_\parallel^0$.

The macroscopic warm-fluid equations are linearized for small-amplitude perturbations, and a single eigenvalue equation is derived for the perturbed electrostatic potential $\delta\phi(\mathbf{x}, t)$, allowing for arbitrary anisotropy in the perpendicular and parallel pressures, $P_\perp^0(r)$ and $P_\parallel^0(r)$. Detailed stability properties are calculated numerically [50] for the case of extreme anisotropy with $P_\parallel^0(r) = 0$ and $P_\perp^0(r) \neq 0$, assuming axisymmetric wave perturbations ($\partial/\partial \theta = 0$) of the form

$\delta\phi(\mathbf{x}, t) = \delta\hat{\phi}(r) \exp(ik_z z - i\omega t)$, where k_z is the axial wavenumber, and $\text{Im } \omega > 0$ corresponds to instability (temporal growth). For $k_z = 0$, the analysis of the eigenvalue equation leads to a discrete spectrum $\{\omega_n\}$ of stable oscillations with $\text{Im } \omega_n = 0$, where n is the radial mode number. On the other hand, for sufficiently large values of $k_z r_b$, where r_b is the beam radius, the analysis of the eigenvalue equation leads to an anisotropy-driven instability ($\text{Im } \omega > 0$) provided the normalized Debye length ($\Gamma_D = \lambda_{D\perp}/r_b$) is sufficiently large and the normalized beam intensity ($s_b = \hat{\omega}_{\text{pb}}^2 / 2\gamma_b^2 \omega_{\beta b}^2$) is sufficiently below the space-charge limit. Here, $\hat{\omega}_{\text{pb}}^2 \equiv 4\pi \hat{n}_b q_b^2 / \gamma_b m_b$ and $\lambda_{D\perp}^2 \equiv 2\hat{T}_{\perp b} \gamma_b^2 / 4\pi \hat{n}_b q_b^2$, where \hat{n}_b and $\hat{T}_{\perp b}$ are the on-axis ($r = 0$) values of density and perpendicular temperature. Depending on system parameters, the growth rate can be a substantial fraction of the focusing frequency $\omega_{\beta b}$ of the applied field [50].

Typical numerical results in the unstable case are illustrated in Figs. 4 and 5. For the choice of waterbag equilibrium considered here with $\hat{T}_{\parallel b} = 0$, the onset of instability occurs for $\Gamma_D > \Gamma_D^* = 0.364$, $s_b < s_b^* = 0.750$, and $v/v_0 > v^*/v_0 = 0.500$, which are equivalent conditions. Here, $v/v_0 \equiv (1 - s_b)^{1/2}$ is a measure of the effective tune depression, and v_0 is undefined by $v_0 \equiv \omega_{\beta b}$. Numerical solutions to the eigenvalue equation [50] are shown in Fig. 4 for the choice of system parameters $\Gamma_D = 0.509$ ($s_b = 0.55$). From Fig. 4, for $0 \leq k_z r_b < k_z^* r_b = 0.968$, the eigenvalue equation supports two real oscillatory solutions with $\text{Im } \omega = 0$. For $k_b r_b > k_z^* r_b = 0.968$, however, the two modes coalesce and have the same value of $\text{Re}(\omega - k_z V_b)$, and complex conjugate values of $\text{Im } \omega$ (one mode is damped, and the other is growing). The normalized growth rate $\text{Im } \omega / v_0$ of the unstable branch is plotted versus $k_z r_b$ in Fig. 4(a), and increases from $\text{Im } \omega = 0$ at $k_z r_b = k_z^* r_b = 0.968$, to $\text{Im } \omega \simeq 0.4v_0$ for $k_z r_b \gg 1$. Consistent with Fig. 4(a), the corresponding eigenfunction plots of $\text{Re}[\delta\hat{\phi}(r)]$ and $\text{Im}[\delta\hat{\phi}(r)]$ versus r/r_b are presented in Fig. 4(b) for $k_b r_b = 4$, corresponding to instability. For moderately low values of $k_z r_b$, the eigenfunction for the unstable mode has the distinctive $n = 1$ mode structure illustrated in Fig. 4(b) for $k_z r_b = 4$. As $k_z r_b$ is increased, however, the real part of the

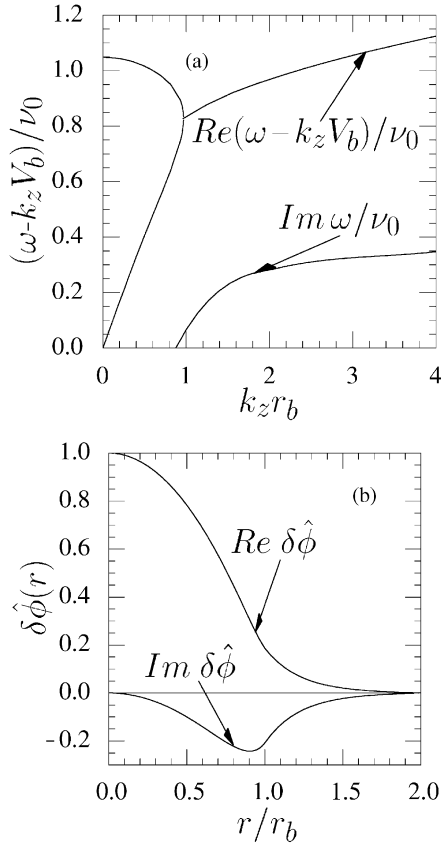


Fig. 4. Plots of (a) $Re(\omega - k_z V_b)/\nu_0$ and $Im \omega/\nu_0$ versus $k_z r_b$, and (b) $Re[\delta \hat{\phi}(r)]$ and $Im[\delta \hat{\phi}(r)]$ versus r/r_b for $k_z r_b = 4$, obtained numerically from the warm-fluid eigenvalue equation for $\Gamma_D = 0.509$ ($s_b = 0.55$).

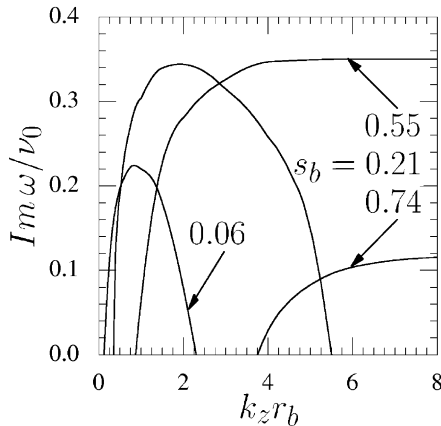


Fig. 5. Plots of $Im \omega/\nu_0$ versus $k_z r_b$ obtained numerically from the warm-fluid eigenvalue equation for several values of $s_b < s_b^* = 0.750$ and $\Gamma_D > \Gamma_D^* = 0.364$.

eigenfunction, $Re[\delta \hat{\phi}(r)]$, changes continuously from an $n = 1$ to an $n = 2$ mode structure [50].

For completeness, shown in Fig. 5 are plots of the normalized growth rate $Im \omega/\nu_0$ versus $k_z r_b$ obtained numerically [50] for several values of $\Gamma_D > \Gamma_D^*$ and $s_b < s_b^*$. Note from Fig. 5 that critical value of $k_z r_b$ for onset of instability increases as Γ_D is increased (s_b is decreased), and that the maximum normalized growth rate $(Im \omega)_{max}/\nu_0$ increases as Γ_D is increased (s_b is decreased). For sufficiently large value of Γ_D (large enough transverse emittance), we also note from Fig. 5 that the instability has a finite bandwidth in $k_z r_b$, whereas for smaller values of Γ_D , the maximum growth rate occurs for $k_z r_b \gg 1$. For $\hat{T}_{b\parallel} \neq 0$ (but $\hat{T}_{b\parallel} < \hat{T}_{b\perp}$), it is expected a numerical solution of the complete eigenvalue equation [50] will always give a finite instability bandwidth in $k_z r_b$.

As a general remark, application of a warm-fluid model to describe the equilibrium and stability properties of intense charged particle beams appears to be a remarkably robust and simple approach, both for the case of stable high-frequency collective oscillations [48], as well as the unstable case considered here, where the instability is driven by gross macroscopic properties of the beam equilibrium (pressure anisotropy) [50].

4. Halo particle production by collective mode excitations in intense charged particle beams

It is important to develop improved theoretical models of halo production and control for charged-particle beam propagation in high-intensity accelerators. Halo production mechanisms [53–58] such as beam mismatch, nonlinearities associated with nonuniform space charge, envelope instabilities, and static field nonlinearities, have met with varying degrees of success, using test-particle and particle-core models, where appropriate. In a recent analysis [58], we describe a new mechanism for halo formation based on collective oscillations excited self-consistently in the charged particle beam. The calculation examines analytically and numerically the effects of collective oscillations on the motion of a test particle in the beam core. Even under ideal

conditions, assuming a constant transverse focusing force (smooth focusing approximation), and axisymmetric (breathing-mode) perturbations about a uniform-density, constant-radius Kapchinskij–Vladimirskij (KV) beam equilibrium, it is found that collective mode excitations, in combination with the applied focusing force and the equilibrium test fields, can eject particles from the beam core to large radii [58].

Collective modes determined from the warm-fluid model of Lund and Davidson [48] allow the derivation of the equations of motion for test ions in the beam interior and exterior regions. Test particle orbits are calculated for collective oscillations with $n = 1$ and 2 radial mode structure, and an estimate is obtained for the range of initial conditions for which particles will be expelled from the beam interior. Resonances for meridional particles are found to be unimportant, while a class of particles with nonzero angular momentum are found to participate in resonant behavior. Once expelled from the beam, numerical solutions of the orbit equations [58] indicate that Kolmogorov–Arnold–Moser surfaces confine particles within 1.5 times the beam radius for moderately low mode amplitudes, but are successively destabilized for higher amplitudes.

As a general remark, the collective oscillations, causing time-dependent forces in the beam interior, can nonresonantly excite particles to higher transverse energies. This enables edge particles, from near the surface of a matched beam, to escape when they would otherwise remain indefinitely confined. The radial extent of expelled particles is determined analytically and numerically, and can be a significant fraction of the beam cross-section near the edge. A similar large effect is observed for collective excitations about a warm-fluid waterbag equilibrium [50] in which the beam density profile decreases monotonically from the beam axis ($r = 0$) to the beam edge ($r = r_b$).

5. Hamiltonian averaging techniques applied to intense beam propagation through alternating-gradient field configurations

As noted earlier, periodic focusing accelerators and transport systems have a wide range of

practical applications. While the Kapchinskij–Vladimirskij (KV) distribution [9,10] is a well-known solution to the nonlinear Vlasov–Maxwell equations for periodic focusing (quadrupole or solenoidal) field configurations, it is nonetheless of very limited practical interest. This is because the (monoenergetic) KV distribution function has a highly inverted (and unphysical) distribution in phase space, and the corresponding density profile is exactly uniform in the beam interior. It is therefore important to develop a framework based on the nonlinear Vlasov–Maxwell equations [1] that is able to investigate the equilibrium and stability properties of a far more general class of periodically focused beam distribution functions. In a recent calculation [26], Channell has developed a third-order Hamiltonian averaging technique for investigating solutions to the nonlinear Vlasov–Maxwell equations for systems subject to a periodic external force. Following the Von Zeipel procedure, the formalism [26] uses a canonical transformation given by an expanded generating function to transform away the rapidly oscillating terms and end up with a Hamiltonian \mathcal{H} that depends only on ‘slow’ variables. In a recent analysis [25], we have applied this averaging technique to intense beam propagation through a periodic focusing lattice. The asymptotic expansion procedure is expected to be valid [25] for sufficiently small phase advance ($\sigma \lesssim 60^\circ$, say).

To briefly summarize, the analysis considers a high-intensity nonneutral beam of positive ions (with charge q_b , and rest mass m_b) propagating in the z -direction with characteristic average axial momentum $\gamma_b m_b \beta_b c$, and directed kinetic energy $(\gamma_b - 1)m_b c^2$. The beam propagates through an applied field that produces a transverse focusing force, $-[\kappa_x(s)x\hat{e}_x + \kappa_y(s)y\hat{e}_y]$, on the beam particles. Here, $V_b = \beta_b c = \text{const.}$ is the average axial velocity, $\gamma_b = (1 - \beta_b^2)^{-1/2}$ is the relative mass factor, c is the speed of light in vacuo, $s = \beta_b ct$ is the axial coordinate, the ion motion in the beam frame is assumed to be nonrelativistic, and the lattice functions, $\kappa_x(s)$ and $\kappa_y(s)$, have axial periodicity length $S = \text{const.}$ Both the cases of a periodic focusing quadrupole field and a periodic focusing solenoidal field are considered [25]. Furthermore, the analysis assumes negligible axial

momentum spread, and the starting point is the nonlinear Vlasov–Maxwell equations for the distribution function $f_b(x, y, x', y', s)$ and (normalized) self-field potential $\psi(x, y, s) = q_b \phi(x, y, s) / \gamma_b^3 m_b \beta_b^2 c^2$ in the transverse phase space (x, y, x', y') in the laboratory frame. Here, for an alternating-gradient quadrupole field with $\kappa_x(s) = -\kappa_y(s) = \kappa_q(s)$, the Hamiltonian for single-particle motion in the laboratory frame is given (in dimensionless units) by

$$\hat{H}(x, y, x', y', s) = \frac{1}{2}(x'^2 + y'^2) + \frac{1}{2}\kappa_q(s)(x^2 - y^2) + \psi(x, y, s) \quad (5)$$

where $\kappa_q(s + S) = \kappa_q(s)$ is the oscillatory lattice function with $\int_0^S ds \kappa_q(s) = 0$. The Hamiltonian \hat{H} is formally assumed to be of order

$$\varepsilon = \frac{\hat{\kappa}_q S^2}{(2\pi)^2} \quad (6)$$

a small dimensionless parameter ($\varepsilon < 1$) proportional to the characteristic strength ($\hat{\kappa}_q$) of the focusing field.

The analysis [25] makes use of Channell's third-order Hamiltonian averaging technique [26] to transform from laboratory-frame variables (x, y, x', y') to a new Hamiltonian $\mathcal{H}(\tilde{X}, \tilde{Y}, \tilde{X}', \tilde{Y}', s)$ in the 'slow' variables $(\tilde{X}, \tilde{Y}, \tilde{X}', \tilde{Y}')$, correct to order ε^3 . The formalism employs a canonical transformation given by an expanded generating function to transform away the rapidly oscillating terms. This leads to a Hamiltonian in the transformed variables of the form

$$\mathcal{H}(\tilde{X}, \tilde{Y}, \tilde{X}', \tilde{Y}', s) = \frac{1}{2}(\tilde{X}'^2 + \tilde{Y}'^2) + \frac{1}{2}\kappa_f(\tilde{X}^2 + \tilde{Y}^2) + \psi(\tilde{X}, \tilde{Y}, s) \quad (7)$$

where $\kappa_f = \text{const.}$ is defined by

$$\kappa_f = \frac{1}{S} \int_0^S ds [\alpha_q^2(s) - \langle \alpha_q \rangle^2] \quad (8)$$

$$\alpha_q(s) = \int_0^s ds \kappa_q(s), \quad \langle \alpha_q \rangle = \frac{1}{S} \int_0^S ds \alpha_q(s).$$

Of course, an important byproduct of the generating function analysis is the determination of the coordinate transformation [25] that relates the laboratory-frame variables (x, y, x', y') to the 'slow' variables $(\tilde{X}, \tilde{Y}, \tilde{X}', \tilde{Y}')$. The major simplification

associated with transforming to the slow variables $(\tilde{X}, \tilde{Y}, \tilde{X}', \tilde{Y}')$ is immediately evident from the expression for $\mathcal{H}(\tilde{X}, \tilde{Y}, \tilde{X}', \tilde{Y}', s)$ in Eq. (7). In particular, the focusing coefficient κ_f is both *constant* (independent of s) and *isotropic* in the transverse plane. This should be contrasted with the expression for the Hamiltonian $\hat{H}(x, y, x', y', s)$ in Eq. (5) in the laboratory frame, where the focusing coefficient $\kappa_q(s)$ is a rapidly oscillating functions of s . Following an analysis of the nonlinear Vlasov–Maxwell equations for $F_b(\tilde{X}, \tilde{Y}, \tilde{X}', \tilde{Y}', s)$ and $\psi(\tilde{X}, \tilde{Y}, s)$ in the transformed variables [25], we present several examples of axisymmetric equilibrium solutions, i.e., distribution functions $F_b^0(\mathcal{H}^0)$ with $\partial/\partial s = 0$ and $\partial/\partial \Theta = 0$, corresponding to beam equilibria with circular cross-section in the transformed variables [16]. Of particular note is the class of distribution functions that satisfy $\partial F_b^0(\mathcal{H}^0)/\partial \mathcal{H}^0 \leq 0$, which can be shown to be *stable* (Section 1). Finally, the inverse coordinate transformation, $\tilde{X}(x, y, x', y', s)$, $\tilde{Y}(x, y, x', y', s)$, etc., has been exploited [25] to determine properties of the *periodically focused* distribution function $f_b(x, y, x', y', s)$ in the laboratory frame correct to order ε^3 , consistent with the class of constant-radius, circular cross-section beam equilibria $F_b^0(\mathcal{H}^0)$ in the transformed variables. A wide range of important physical quantities are determined, including the distribution function $f_b(x, y, x', y', s)$; statistical averages such as the transverse mean-square beam dimensions, $\langle x^2 \rangle(s)$ and $\langle y^2 \rangle(s)$, and the unnormalized transverse emittances, $\varepsilon_x(s)$ and $\varepsilon_y(s)$; and macroscopic properties such as the number density of beam particles, $n_b(x, y, s) = \int dx' dy' f_b(x, y, x', y', s)$, the self-field potential, $\psi(x, y, s)$, etc.

To summarize, this formalism [25] represents a powerful framework for investigating the equilibrium and stability properties of an intense beam propagating through an alternating-gradient quadrupole field. First, the analysis applies to a broad class of distributions $F_b^0(\mathcal{H}^0)$ in the transformed variables. Second, the determination of (periodically focused) beam properties in the laboratory frame is straightforward. Third, the analysis applies to beams with arbitrary space-charge intensity, consistent only with requirement for radial confinement of the

beam particles by the applied focusing field ($\kappa_f \beta_b^2 c^2 > \hat{\omega}_{pb}^2 / 2\gamma_b^2$). Finally, the formalism can be extended in a straightforward manner to the case of a periodic-focusing solenoidal field $\mathbf{B}_{\text{sol}}(\mathbf{x}) = B_z(s)\hat{\mathbf{e}}_z - (1/2)B'_z(s)(x\hat{\mathbf{e}}_x + y\hat{\mathbf{e}}_y)$ [25], and to the case where weak nonlinear corrections to the transverse focusing force are retained in the analysis.

6. Conclusions

In this paper, we have summarized highlights of selected heavy ion fusion research activities carried out at the Princeton Plasma Physics Laboratory since the 1997 Heidelberg symposium on heavy ion fusion [7], with particular emphasis on analytical and numerical simulation studies of collective processes in intense beam propagation. The work summarized here has included development of a three-dimensional stability theorem for intense beam propagation based on the nonlinear Vlasov–Maxwell equations (Section 1); analytical and numerical studies of the electron–ion two-stream instability in high-intensity ion beams (Section 2); warm-fluid investigations on collective instabilities driven by pressure anisotropy in intense charged particle beams (Section 3); studies of halo particle production by collective mode excitations (Section 4); and the development of Hamiltonian averaging techniques for describing intense beam propagation through periodic focusing field configurations (Section 5). Important theoretical advances have been made in each of these areas, and a notable characteristic of the work reported here is the strong interplay between analytical studies and numerical analysis and simulation, which is essential to develop a predictive capability for modeling present- and next-generation heavy ion fusion experiments.

Acknowledgements

This research was supported by the U.S. Department of Energy.

References

- [1] R.C. Davidson, *Physics of Nonneutral Plasmas*, Addison-Wesley Publishing Co., Reading MA, 1990, and references therein.
- [2] A.W. Chao, *Physics of Collective Beam Instabilities in High Energy Accelerators*, Wiley, New York, 1993.
- [3] M. Reiser, *Theory and Design of Charged Particle Beams*, Wiley, New York, 1994.
- [4] D.A. Edwards, M.J. Syphers, *An Introduction to the Physics of High-Energy Accelerators*, Wiley, New York, 1993.
- [5] T.P. Wangler, *Principles of RF Linear Accelerators*, Wiley, New York, 1998.
- [6] J.D. Lawson, *The Physics of Charged-Particle Beams*, Oxford Science Publications, New York, 1988.
- [7] I. Hofmann (Ed.), *Proceedings of the 1997 International Symposium on Heavy Ion Inertial Fusion*, Nucl. Instr. and Meth. 415 (1998) 1, and references therein.
- [8] J.J. Barnard, T.J. Fessenden, E.P. Lee (Eds.), *Proceedings of the 1995 International Symposium on Heavy Ion Inertial Fusion*, J. Fusion Eng. Des. 32 (1996) 1, and references therein.
- [9] I. Kapchinskij, V. Vladimirkij, *Proceedings of the International Conference on High Energy Accelerators and Instrumentation*, CERN Scientific Information Service, Geneva, 1959, p. 274.
- [10] R.L. Gluckstern, in: M.R. Tracy (Ed.), *Proceedings of the 1970 Proton Linear Accelerator Conference*, Batavia, IL, National Accelerator Laboratory, Batavia, IL, 1971, p. 811.
- [11] T.-S. Wang, L. Smith, *Part. Accel.* 12 (1982) 247.
- [12] I. Hofmann, L.J. Laslett, L. Smith, I. Haber, *Part. Accel.* 13 (1983) 145.
- [13] I. Hofmann, J. Struckmeier, *Part. Accel.* 21 (1987) 69.
- [14] J. Struckmeier, I. Hofmann, *Part. Accel.* 39 (1992) 219.
- [15] N. Brown, M. Reiser, *Phys. Plasmas* 2 (1995) 969.
- [16] R.C. Davidson, C. Chen, *Part. Accel.* 59 (1998) 175.
- [17] R.C. Davidson, W.W. Lee, P.H. Stoltz, *Phys. Plasmas* 5 (1998) 279.
- [18] R.C. Davidson, *Phys. Rev. Lett.* 81 (1998) 991.
- [19] R.C. Davidson, *Phys. Plasmas* 5 (1998) 3459; W. Newcomb, as reported by I.B. Bernstein, *Phys. Rev.* 109 (1958) 10; C.S. Gardner, *Phys. Fluid* 6 (1963) 839; R.C. Davidson, N.A. Krall, *Phys. Fluids* 13 (1970) 1543.
- [20] P.H. Stoltz, R.C. Davidson, W.W. Lee, *Phys. Plasmas* 6 (1999) 298.
- [21] W.W. Lee, Q. Qian, R.C. Davidson, *Phys. Lett. A* 230 (1997) 347.
- [22] Q. Qian, W.W. Lee, R.C. Davidson, *Phys. Plasmas* 4 (1997) 1915.
- [23] A. Friedman, D.P. Grote, *Phys. Fluids B* 4 (1992) 2203.
- [24] A. Friedman, J.J. Barnard, D.P. Grote, I. Haber, *Nucl. Instr. and Meth. A* 415 (1998) 455.
- [25] R.C. Davidson, H. Qin, P.J. Channell, *Phys. Rev. Special Top. Accel. Beams* 2 (1999) 074401, 3 (2000) 029901.
- [26] P.J. Channell, *Phys. Plasmas* 6 (1999) 982; 3 (2000) 029901.

- [27] D. Neuffer, E. Colton, D. Fitzgerald, T. Hardek, R. Hutson, R. Macek, M. Plum, H. Thiessen, T.-S. Wang, Nucl. Instr. and Meth. A 321 (1992) 1.
- [28] D. Neuffer, C. Ohmori, Nucl. Instr. and Meth. A 343 (1994) 390.
- [29] D. Sagan, A. Temnykh, Nucl. Instr. and Meth. A 344 (1994) 459.
- [30] M. Izawa, Y. Sato, T. Toyomasu, Phys. Rev. Lett. 74 (1995) 5044.
- [31] S.A. Heifets, Transverse instability driven by trapped electrons, Stanford Linear Accelerator Center Report SLAC/AP-95-101, 1995.
- [32] T.O. Roubenheimer, F. Zimmermann, Phys. Rev. E52 (1995) 5487; G.V. Stupakov, T.O. Roubenheimer, F. Zimmermann, Phys. Rev. E52 (1995) 5499.
- [33] J. Byrd, A. Chao, S. Heifets, M. Minty, T.O. Roubenheimer, J. Seeman, G. Stupakov, J. Thomson, F. Zimmermann, Phys. Rev. Lett. 79 (1997) 79.
- [34] K. Ohmi, Phys. Rev. E55 (1997) 7550.
- [35] P.A. Seidl, C.M. Celata, W.W. Chupp, A. Faltens, W.M. Fawley, W. Ghiorso, K. Hahn, E. Henestroza, S. MacLaren, C. Peters, D.P. Grote, I. Haber, Nucl. Instr. and Meth. A 415 (1998) 243.
- [36] C.M. Celata, W. Chupp, A. Faltens, W.M. Fawley, W. Ghiorso, K.D. Hahn, E. Henestroza, D. Judd, C. Peters, P.A. Seidl, Fusion Eng. Des. 32 (1996) 219.
- [37] R. Macek, Proceedings of the Workshop on Space-Charge Physics in High-Intensity Hadron Rings, American Institute of Physics Conference Proceedings, Vol. 448, 1998, p. 116.
- [38] R.C. Davidson, H. Qin, G. Shvets, Phys. Plasmas 7 (2000), in press.
- [39] H. Qin, R.C. Davidson, W.W. Lee, Proceedings of the 1999 Particle Accelerator Conference, Vol. 3, 1999, p. 1626.
- [40] H. Qin, R.C. Davidson, W.W. Lee, American Institute of Physics Conference Proceedings, Vol. 496, 1999, p. 295.
- [41] H. Qin, R.C. Davidson, W.W. Lee, Phys. Lett. A 272 (2000) 389.
- [42] R.C. Davidson, H. Qin, P.H. Stoltz, T.-S. Wang, Phys. Rev. Special Top. Accel. Beams 2 (1999) 054401, and references therein.
- [43] R.C. Davidson, H. Qin, T.-S. Wang, Phys. Lett. A 252 (1999) 213.
- [44] R.C. Davidson, H. Qin, Phys. Lett. A 270 (2000) 177.
- [45] R.C. Davidson, H. Qin, I. Kaganovich, W.W. Lee, Stabilizing influence of axial momentum spread on the two-stream instability in intense heavy ion beams, Nucl. Instr. and Meth. A 464 (2001) 493, these proceedings .
- [46] R.C. Davidson, P. Stoltz, C. Chen, Phys. Plasmas 4 (1997) 3710.
- [47] I. Hofmann, Phys. Rev. E57 (1998) 4713.
- [48] S.M. Lund, R.C. Davidson, Phys. Plasmas 5 (1998) 3028.
- [49] C. Chen, R. Pakter, Phys. Plasmas 7 (2000), in press.
- [50] R.C. Davidson, S. Strasburg, Phys. Plasmas 7 (2000) 2657.
- [51] I. Haber, D.A. Callahan, A. Friedman, D.P. Grote, S.M. Lund, T.-S. Wang, Nucl. Instr. and Meth. A 415 (1998) 345.
- [52] S.M. Lund, D.A. Callahan, A. Friedman, D.P. Grote, I. Haber, T.-S. Wang, Theory of an electrostatic instability driven by transverse-longitudinal temperature anisotropy in space-charge-dominated beams, Proceedings of the 19th International Linac Conference, Chicago, IL, 1998.
- [53] S.Y. Lee (Ed.), Space Charge Dominated Beams and Applications of High Brightness Beams, American Institute of Physics Conference Proceedings, Vol. 377, American Institute of Physics, New York, 1996, and references therein.
- [54] J. Lagniel, Nucl. Instr. and Meth. 345 (1994) 46.
- [55] R. Gluckstern, W. Cheng, H. Ye, Phys. Rev. Lett. 75 (1995) 2835.
- [56] R. Gluckstern, Phys. Rev. Lett. 73 (1994) 1247.
- [57] C. Chen, R. Pakter, R.C. Davidson, Phys. Plasmas 6 (1999) 3647.
- [58] S. Strasburg, R.C. Davidson, Phys. Rev. E61 (2000) 5753.